







Comparative Investigations on the Bioactivity of Surface Grain Refined Titanium and Surface Oxidized Titanium for Biomedical Implant Applications

Chelamalasetti Pavan Satyanarayana ^{1,*}, Lam Suvana Raju ¹, Lam Ratna Raju ¹, Sreekanth Dondapati ², Ravikumar Dumpala ³, Ratna Sunil Buradagunta ^{4,*}

¹ Department of Mechanical Engineering, Vignan's Foundation for Science, Technology & Research, Vadlamudi 522213, India; chpavansatyanarayana@gmail.com (Ch.P.S.), rajumst@gmail.com (L.S.R.), lamratnaraju@gmail.com (L.R.R.);

² School of Mechanical Engineering, Vellore Institute of Technology, Chennai 600127, India, sreekanth.dondapati@vit.ac.in (SD);

³ Department of Mechanical Engineering, Visvesvaraya National Institute of Technology, Nagpur 440010, India; ravikumardumpala@mec.vnit.ac.in (RKD);

⁴ Department of Mechanical Engineering, Bapatla Engineering College, Bapatla 522101, India; bratnasunil@gmail.com (RSB);

* Correspondence: chpavansatyanarayana@gmail.com (C.P.S.); bratnasunil@gmail.com (R.S.B.);

Scopus Author ID35410353400

Received: 3.06.2022; Accepted: 7.07.2022; Published: 11.09.2022

Abstract: Surface engineering of titanium (Ti) for medical implant applications is an active research area in the biomedical field across the globe. Improving the bioactivity of the Ti surface is crucial for implant applications where osseointegration is essentially required to enhance the healing rate. In the present work, shot peening followed by micro-arc oxidation (MAO) treatments were applied to pure Ti with an objective to investigate the role of surface grain refinement and the oxide layer on biomineralization ability to assess the bioactivity of the surface. After shot peening with steel balls, Ti substrates were subjected to MAO using sodium phosphate solution. Grain refinement was observed at the surface after the shot peening at a submicrometer levels ranging from 0.5 to 2 μm for a thickness of $\sim 50\mu\text{m}$. Ti sheets subjected to MAO exhibited a porous oxide layer on the surface. From the XRD analysis, the TiO_2 layer was observed as a combination of anatase and rutile. Higher Ca/P-based apatite deposition on shot-peened Ti compared with MAO Ti was observed in the *in vitro* immersion studies. The results indicated increased bioactivity for grain refined Ti compared with MAO Ti. Hence, it is concluded that the microstructure influences the bioactivity of Ti implants compared with the oxide layer.

Keywords: Ti implant; micro-arc oxidation; shot peening; bioactivity; biomineralization; implant tissue interface.

© 2022 by the authors. This article is an open-access article distributed under the terms and conditions of the Creative Commons Attribution (CC BY) license (<https://creativecommons.org/licenses/by/4.0/>).

1. Introduction

Tailoring the surface of titanium (Ti) to enhance its surface properties through different surface engineering methods, including coatings and surface treatments, is an active area of research in biomedical engineering. Being a relatively lightweight material compared with steels and Co alloys, Ti reduces the stress shielding issue usually found in load-bearing medical implants [1, 2]. Diagnosis by MRI scanning is also conveniently carried out for patients with Ti implants, unlike the other metallic implants. High corrosion resistance and better compatibility in the physiological environment make Ti a promising implant material [3, 4].

However, the lack of osseointegration is a limitation of the bare Ti surface. Higher osseointegration is desirable in developing implants for artificial joints and dental implants [5-7]. Ti exhibits bio-inert nature; hence, appropriate surface treatment is adopted, or a coating is provided to make Ti surface bioactive or introduce antimicrobial properties [3]. It is evidently explained that grain size significantly alters the structure-sensitive properties of materials. It is understood from the available scientific literature that fine-grained Ti promotes better tissue implant interactions [8-16]. Since the implant surface properties govern the bio interactions at the tissue-implant interface, refining the microstructure at the surface can enhance the bioactivity of Ti implants.

In the shot peening process, a number of tiny balls are used to bombard the surface to introduce higher compressive stresses. Usually, the surfaces of engineering components are treated with shot peening to increase the fatigue life of engineering components [17-19]. Surface grain refinement can also be achieved in shot peening [20]. The grain refinement to a level of nano-ultra fine-grained structure promotes higher bioactivity [21]. On the other hand, micro-arc oxidation ((MAO) is another surface engineering process in which a self-grown porous oxide layer can be developed from the metallic surface by using an appropriate electrolyte [22]. Several earlier reports demonstrated the development of the TiO₂ on Ti substrate by MAO process for implant applications [23-26]. Furthermore, several biocompatible elements were also embedded into TiO₂ during MAO to functionalize the Ti substrate with antimicrobial properties [27-29]. Usually, the electrochemical events at the fine-grained surfaces are rapid compared with coarse-grained surfaces [9, 30]. Therefore, grain refinement influences the rate of oxidation of Ti. Hence, in the present work, the grain-refined Ti surface was produced by shot peening, and both the grain-refined and base Ti samples were subjected to the MAO process. Then the samples were subjected to *in vitro* studies in artificial body fluids to understand the effect of refined microstructure and oxide layer on enhancing the bioactivity of Ti.

2. Materials and Methods

Pure titanium (Ti) sheets (medical grade) of thickness 2 mm were obtained from Venku Metals, India. Shot peening experiments were conducted on sheets of area 100 x 100 mm² by using steel balls of diameter 2 mm. Pressurized air was used to strike the substrate with the steel balls through a nozzle, as shown in Figure 1(a), for 5 min. The balls induce localized compressive stress that leads to the development of fine grains at the surface, as schematically illustrated in Figure 1(a). Both the base material (Ti) and shot-peened Ti (SP-Ti) were subjected to micro-arc oxidation (MAO) by using sodium phosphate solution as the electrolyte. Fig 1(b) presents the schematic drawing of the MAO process in which platinum was used as the counter electrode. MAO process was done at a voltage of 240 V by applying a current density of 250 mN/cm² for 10 min. After the MAO process, the samples were named as follows, Ti MAO and SP-Ti MAO for base material and shot-peened Ti, respectively.

For microstructural studies, Ti and SP-Ti samples were prepared following a standard protocol to produce mirror-finished surfaces and etched with Kroll's reagent. An inverted optical microscope (Leica, Germany) was used to record the microstructures. A cross-sectional image was observed for the SP-Ti sample. The refined grain surface and MAO processed surfaces were studied by scanning electron microscopy (SEM, TESCON, Czech Republic). The MAO samples were also analyzed for phase analysis by energy-dispersive X-ray

spectroscopy (EDS). Then all the samples were analyzed by X-Ray diffraction (XRD, Bruker, USA) between 20 to 80 ° 2 θ range with a 0.05 step size.

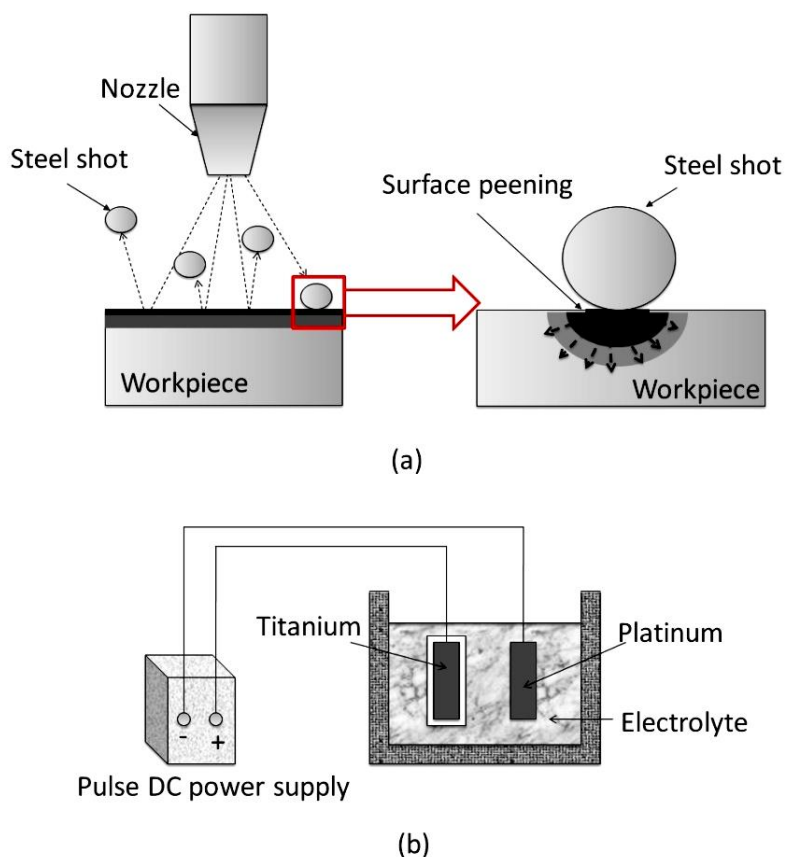


Figure 1.(a) Schematic diagram explaining the shot peening process; (b) Schematic illustration of micro-arc oxidation (MAO) process.

Simulated body fluid (SBF) has been used for *in vitro* bioactivity study. SBF is an artificial physiological solution prepared in the laboratory that has a concentration of ions similar to that of the human extracellular matrix, including Na⁺, K⁺, Mg²⁺, Ca²⁺, Cl⁻, HCO₃⁻, HPO₄²⁻, and SO₄²⁻. In the process of biomaterials evaluation, the materials are immersed in SBF, and the potential of deposition of mineral phases from SBF to the surface of the test material is evaluated to assess the level of bioactivity. Usually, Ca/P mineral phases are formed from the SBF and deposited on the surface of the immersed material. Higher deposition of the Ca-based phases on the surface of the immersed sample indicates the higher bioactivity of the material. The list of required chemicals and their weights, sequence of steps involved in the preparation of SBF, and ion concentration can be referred to from the works of Kokubo *et al.* [31]. The samples for immersion studies were placed in 50 mL of SBF containers and maintained at 37 °C for 28 days. All the immersed samples were then gently washed in water and subjected to XRD, SEM, and EDS analysis.

3. Results and Discussion

The shot peening process introduces grain refinement at the surface, similar to the surface mechanical attrition treatment [32]. Figure 2 shows the microstructures of the samples before and after shot peening. From the linear intercept method, the grain size of the starting material was obtained as 57 ± 2.5 μm. From the cross-sectional image of SP-Ti, it is evident that the shot peening process refined the surface microstructure up to a depth of ~ 50 μm, as

indicated with an arrow in Figure 2(b). SEM image of SP-Ti demonstrates the level of grain refinement due to the shot peening. It can be learned from the microstructure that the refinement of the microstructure happened at different levels, as reflected from 0.5 to 2 μm grain size in the SP-Ti. The level of grain refinement was observed from submicrometer to ultra-fine grain size.

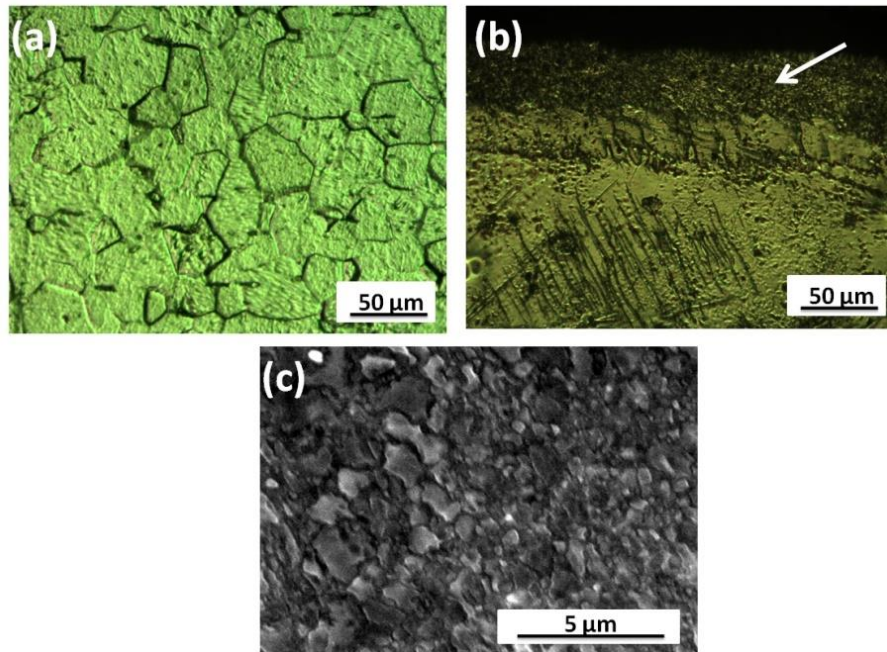


Figure 2. Microstructural observations: a) Ti, b) cross-section of SP-Ti, and c) SEM image of refined grain surface of SP-Ti.

Figure 3 presents the surface morphologies and EDS analysis of MAO samples. The formation of numerous pores in the TiO_2 surface layer is evident in both Ti MAO and SP-Ti MAO samples. It is the characteristic of the MAO process to produce surface layer oxide with porosity. Ti has shown large pores (Figure 3 (a) and (b)) compared with SP-Ti samples (Figure 3(d) and (e)). In SP-Ti, numerous pores of smaller size appeared in the produced TiO_2 layer. The difference in the morphologies of the oxide layer in Ti and SP-Ti can be claimed to be the grain refinement in SP-Ti. Usually, the surfaces with grain refinement exhibit high energy. Therefore, electrochemical events such as corrosion and oxidation are higher under the same environmental conditions [9]. In the present work, the surface of SP-Ti was observed with more surface undulations and porosity. These features are more favorable for cell interactions at the implant tissue interface [33]. From the EDS analysis presence of Ti, P, and O elements were observed for both the MAO samples (Figure 3(c) and (f)). The appearance of Ti and O can be understood from the formation of the TiO_2 layer. Despite gently washing the MAO samples in distilled water after the MAO process, the presence of phosphorous in the TiO_2 layer in both the MAO samples indicates the leftover phosphorous residue from the electrolyte solution after the MAO process. Phosphorous is a biocompatible element and does not cause any toxic issues. Hence, the presence of P in the TiO_2 layer after MAO can be considered an additional advantage.

The XRD patterns of Ti and SP-Ti are presented in Figure 4(a), and XRD plots of Ti MAO and SP-Ti MAO samples are shown in Figure 4 (b). It is evident from the XRD of Ti, and SP-Ti samples (Figure 4 (a)) that the peak intensities of (100), (101), (110), (112), and (201) were observed as decreased, and the peak intensities of (002) and (103) were observed as increased due to shot peening. Usually, the change in the peak intensities is referred to as the

texture change in crystalline materials. In *hcp* metals, the (002) plane is close-packed, and in the present work, it is understood that the SP-Ti has a preferred texture after shot peening. Peak broadening is another significant observation from the XRD pattern of SP-Ti compared with Ti. Usually, peak broadening results in decreased crystallite size. Therefore, the XRD analysis suggests grain refinement in SP-Ti and supports the microstructural findings.

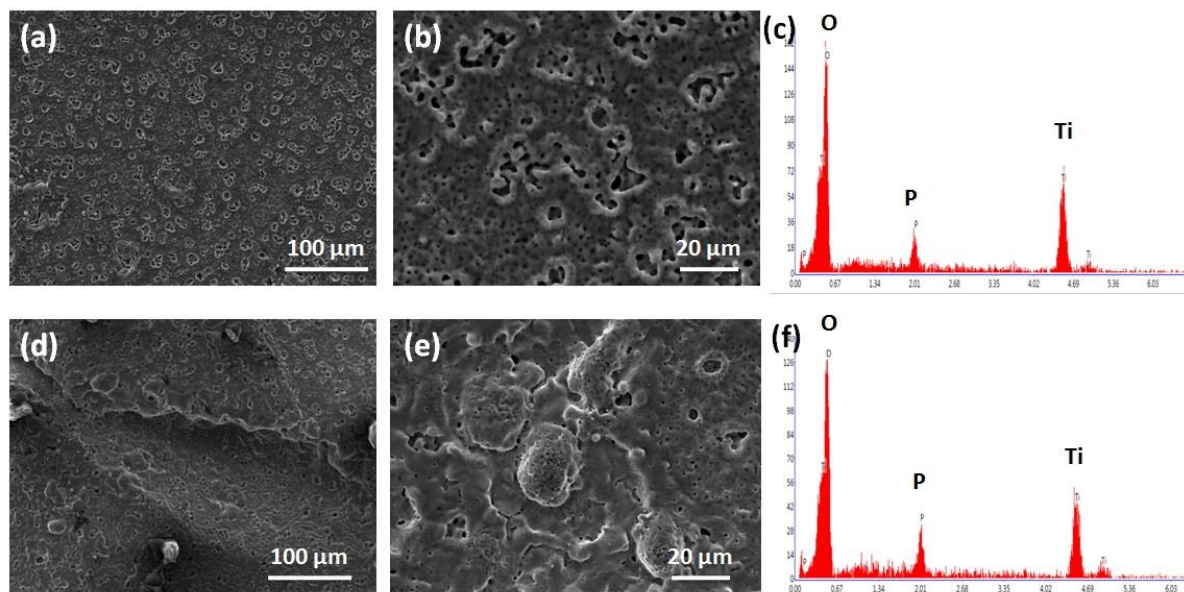


Figure 3. SEM observations of MAO samples: (a) Ti MAO; (b) magnified image of Ti MAO; (c) EDS analysis of Ti-MAO; (d) SP-Ti MAO; (e) magnified image of SP-Ti MAO; (f) EDS analysis of SP-Ti MAO.

The XRD patterns of MAO samples (Figure 4b) show dominating intensities for the TiO_2 phase compared with the base Ti. Interestingly, the developed TiO_2 layer was observed with two phases, i.e., anatase and rutile phases, as indexed in the XRD patterns of Ti MAO and SP-Ti MAO samples (Figure 4 (b)). Usually, TiO_2 exhibits polymorphism and may present in the form of an anatase or rutile phase. The stability of the anatase phase of TiO_2 is lower compared with the rutile phase, as explained in the literature [34, 35]. Hence, in the MAO process, the TiO_2 anatase phase is initially developed, and with the increased process time, the fraction of TiO_2 phase transformation from anatase to rutile is increased [36]. In the present work, both the TiO_2 phases (anatase and rutile) were identified in addition to Ti peaks in Ti MAO and SP-Ti MAO samples. The highest intensity peak, (002) was noticed in the XRD plots of both the Ti MAO and SP-Ti MAO samples. The other peaks corresponding to Ti have not appeared for the samples after MAO. Since the surface TiO_2 layer developed during MAO has completely covered the Ti substrate, XRD peaks corresponding to TiO_2 have dominated, and therefore, intensities of XRD peaks corresponding to Ti were significantly decreased.

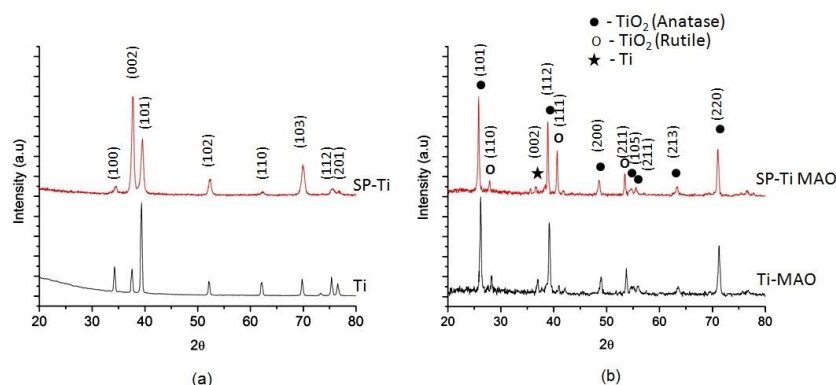


Figure 4. XRD analysis of the samples: (a) Ti and SP-Ti; (b) Ti-MAO and SP-Ti M.A.O.

Figure 5 presents the surface morphologies of the immersed samples collected after 28 days from SBF and their area EDS analysis. From the surface of Ti (Figure 5 (a)), no significant phases were observed as deposited from the SBF. The EDS spectrum (Figure 5 (b)) shows Ti and indicates lower amounts of Ca, P, and O on the sample surface. On the surface of SP-Ti (Figure 5 (c)), the presence of white precipitates deposited from the SBF was noticed, and the EDS analysis (Figure 5 (d)) demonstrates a similar chemical composition to that of the Ti sample. However, relatively more Ca and P suggests the increased bioactivity on the SP-Ti as reflected from the more Ca/P phases deposited from the SBF. The surface morphologies of MAO samples (Figure 5 (e) and (g)) indicate no significant biomineralization on the surfaces. However, the appearance of Ca and P in the EDS analysis (Figure 5 (f)) suggests the deposition of Ca/P phases on the surface of MAO samples.

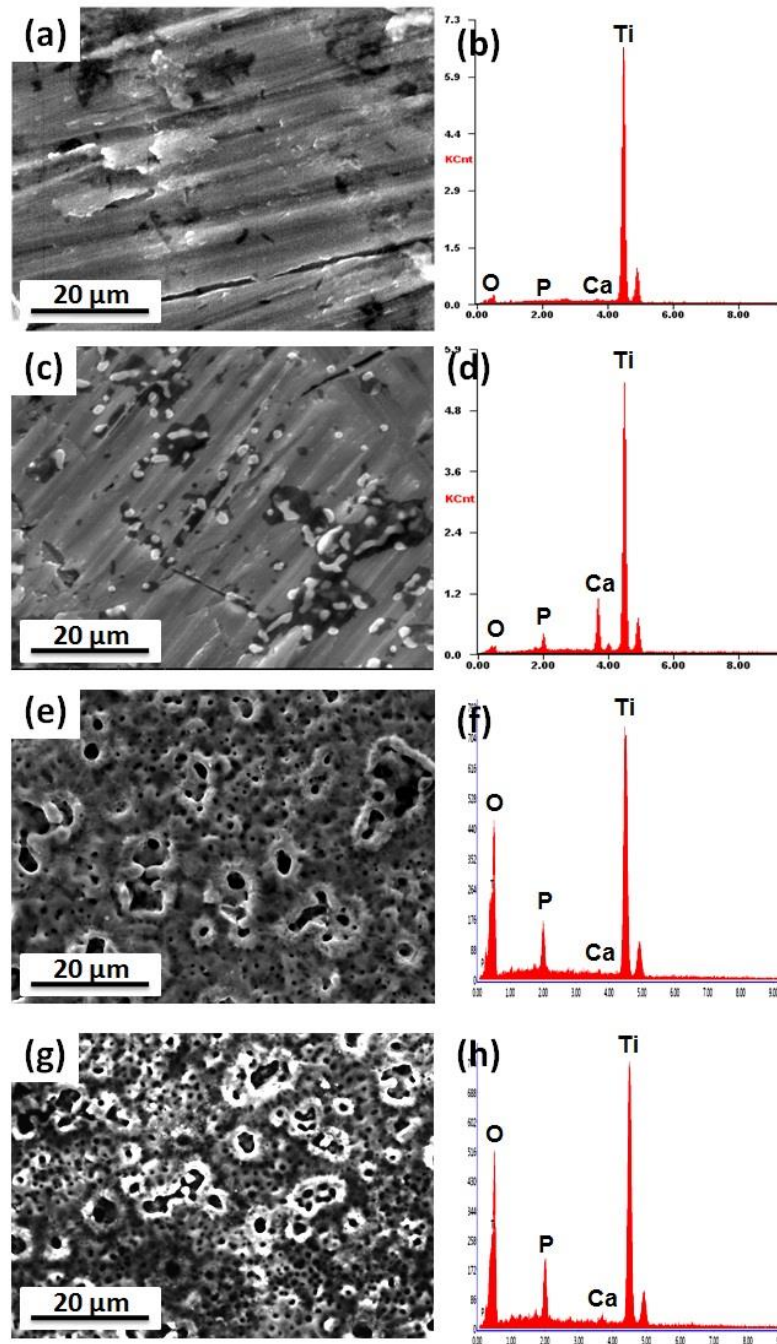


Figure 5. SEM images and obtained EDS spectra of the samples after immersing in SBF solution for 28 days: (a) T; (b) EDS of Ti; (c) SP-Ti; (d) EDS of SP-Ti; (e) Ti MAO; (f) EDS of Ti MAO; (g) SP-Ti MAO; (h) EDS of SP-Ti MAO.

Interestingly, more phosphorous was observed on the Ti MAO and SP-Ti MAO samples. This can be attributed to the presence of phosphorous in the TiO₂ layer before the immersion study. Figure 6 presents the XRD plots of the immersed samples. Even though the presence of Ca and P was observed on the sample surfaces, no significant peak corresponding to any Ca/P phase was observed on the samples except for SP-Ti. A smaller intensity peak corresponding to hydroxyapatite was noticed on SP-Ti at around 31.8°, suggesting the SP-Ti surface's higher bioactivity than the other samples. It is true that the smaller amounts may not be detected in XRD as observed in the case of Ti, Ti MAO, and SP-Ti MAO. The presence of smaller amounts of Ca and P has not been seen in the XRD in the form of any phase. However, smaller amounts of Ca and P on Ti, Ti MAO, and SP-Ti MAO indicate biomineralization in lower concentrations. Among all the samples, higher biomineralization was observed for the SP-Ti sample.

In the context of cell interactions at the implant-tissue interface, MAO surfaces have demonstrated better performance, as learned from the literature [23, 24]. The pores and surface bio-mimicking features resulting in the MAO process are favorable to osseointegration. In the present work, the oxide layer obtained on SP-Ti MAO has more tiny pores and surface undulations than the Ti MAO sample, which is attributed to the fine grain structure achieved by shot peening that accelerated the electrochemical events at the surface. However, from the immersion studies in SBF, higher mineral deposition was observed for the SP-Ti sample due to the grain refinement compared with the MAO samples. This observation can be justified by understanding grain refinement's positive role in increasing surface energy and promoting biomineralization [9, 37, 38]. Hence, the results demonstrate higher biomineralization for the grain refined Ti compared with the ceramic layer of TiO₂ produced by MAO. Therefore, selecting appropriate surface treatment based on the targeted application is crucial to benefit from the surface-functionalized Ti in bone-implant applications.

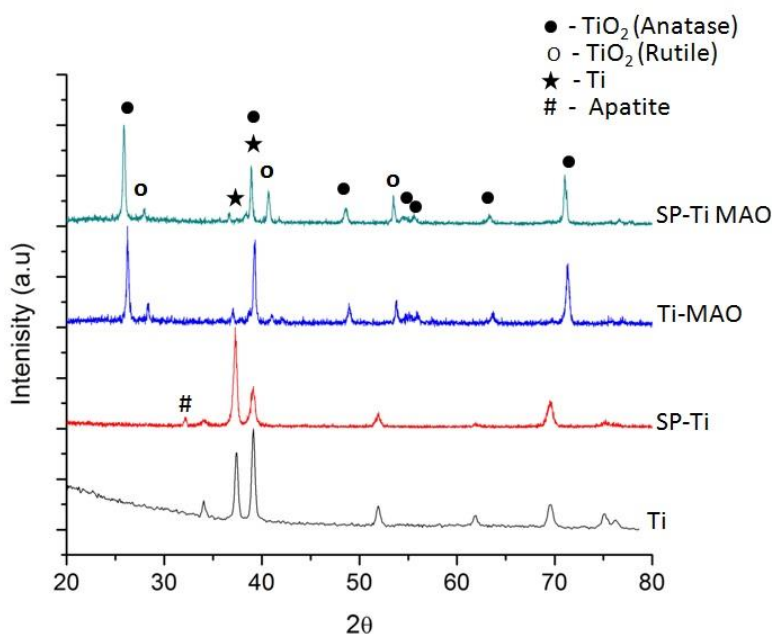


Figure 6. XRD analysis of the immersed samples.

4. Conclusions

Pure Ti was subjected to shot peening to produce a refined grain surface and subsequently subjected to micro-arc oxidation (MAO) to develop a porous TiO₂ layer. A

significant grain refinement up to a level of 0.5 to 2 μm was obtained at the surface of shot-peened Ti for a depth of approximately 50 μm . XRD analysis indicated the development of preferred texture after shot peening dominated with basal (002) texture. The produced submicrometer to ultra-fine grain size microstructure at the surface of Ti led to the developing TiO_2 layer with very fine pores with numerous surface undulations, which favors the implant tissue interactions. From the *in vitro* experiments, a higher level of biomineralization was observed on grain-refined Ti compared with MAO samples, as confirmed by the presence of more Ca/P phases from the SEM and XRD analysis. The present study demonstrates the potential of grain refinement in enhancing biomineralization, which promotes the healing rate compared with the ceramic TiO_2 layer. However, an appropriate route can be selected based on the targeted application where biomineralization is crucial for implant-tissue bonding.

Funding

This research received no external funding.

Acknowledgments

The authors would like to thank Dr. M. Ananda Rao, Principal Scientist, CSIR-National Metallurgical Laboratory, Chennai, India, and Mr. B. Venkateswarlu, Assistant Professor, Dept of Metallurgical and Materials Engineering, RGUKT Nuzvid, India, for providing material testing facilities. The authors also gratefully acknowledge the CoEAMMPC, Vignan University, Vadlamudi, India, for material characterization.

Conflicts of Interest

The authors declare no conflict of interest.

References

1. Zhang, L.C.; Chen, L.Y. A Review on biomedical titanium alloys: recent progress and prospect. *Adv Eng Mater* **2019**, *21*, 1801215, <https://doi.org/10.1002/adem.201801215>.
2. Sarraf, M.; Rezvani Ghomi, E.; Alipour, S.; Ramakrishna, S.; Liana Sukiman, N. A state-of-the-art review of the fabrication and characteristics of titanium and its alloys for biomedical applications. *Bio-des Manuf* **2022**, *5*, 371–395, <https://doi.org/10.1007/s42242-021-00170-3>.
3. Ratna Sunil, B.; Sandeep Kranthi Kiran, A.; Ramakrishna, S. Surface functionalized titanium with enhanced bioactivity and antimicrobial properties through surface engineering strategies for bone implant applications, *Curr Opin Biomed Eng* **2022**, *23*, 100398, <https://doi.org/10.1016/j.cobme.2022.100398>.
4. Kaur, M.; Singh, K. Review on titanium and titanium based alloys as biomaterials for orthopaedic applications. *Mater Sci Eng: C* **2019**, *102*, 844–862, <https://doi.org/10.1016/j.msec.2019.04.064>.
5. Jemat, A.; Ghazali, M.J.; Razali, M.; Otsuka, Y. Surface modifications and their effects on titanium dental implants. *Bio Med Research Intl* **2015**, *2015*, 791725, <https://doi.org/10.1155/2015/791725>.
6. Lu, X.; Wu, Z.; Xu, K.; Wang, X.; Wang, S.; Qiu, H.; Li, X.; Chen, J. Multifunctional coatings of titanium implants toward promoting osseointegration and preventing infection: recent developments. *Front Bioeng Biotechnol* **2021**, *9*, 783816, <https://doi.org/10.3389/fbioe.2021.783816>.
7. Suntharavel Muthaiah, V.M.; Indrakumar, S.; Suwas, S.; Chatterjee, K. Surface engineering of additively manufactured titanium alloys for enhanced clinical performance of biomedical implants: A review of recent developments. *Bioprinting* **2022**, *25*, e00180, <https://doi.org/10.1016/j.bprint.2021.e00180>.
8. Truong, V.K.; Stuart, R.; Lapovok, R.; Estrin, Y.; Wang, J.Y.; Berndt, C.C.; Barnes, D.G.; Fluke, C.J.; Crawford, R.J.; Ivanova, E.P. Effect of ultra fine-grained titanium surfaces on adhesion of bacteria. *Appl Microbiol Biotechnol* **2009**, *83*, 925–937, <https://doi.org/10.1007/s00253-009-1944-5>.

9. Ratna Sunil, B.; Thirugnanam, A.; Chakkingal, U.; Sampath Kumar, T.S. Nano and ultra fine grained metallic biomaterials by severe plastic deformation techniques. *Mater Technol* **2016**, *31*, 743-755, <https://doi.org/10.1080/10667857.2016.1249133>.
10. Wang, Q.; Zhou, P.; Liu, S.; Attarilar, S.; Ma, R.L.; Zhong, Y.; Wang, L. Multi-scale surface treatments of titanium implants for rapid osseointegration: a review. *Nanomaterials* **2020**, *10*, 1244, <https://doi.org/10.3390/nano10061244>.
11. Romero-Resendiz, L.; Gómez-Sáez, P.; Vicente-Escuder, A.; Amigó-Borrás, V. Development of Ti-In alloys by powder metallurgy for application as dental biomaterial. *J Mater Res Technol* **2021**, *11*, 1719-1729, <https://doi.org/10.1016/j.jmrt.2021.02.014>.
12. Dzogbewu, T.C.; du Preez, W.B. Additive manufacturing of titanium-based implants with metal-based antimicrobial agents. *Metals* **2021**, *11*, 453, <https://doi.org/10.3390/met11030453>.
13. Merker, D.; Handzhiyski, Y.; Merz, R.; Kopnarski, M.; Reithmaier, J.P.; Popov, C.; Apostolova, M.D. Influence of surface termination of ultrananocrystalline diamond films coated on titanium on response of human osteoblast cells: a proteome study. *Mater Sci Eng C* **2021**, *128*, 112289, <https://doi.org/10.1016/j.msec.2021.112289>.
14. Nicholson, J.W. Titanium alloys for dental implants: A review. *Prosthesis* **2020**, *2*, 100-116, <https://doi.org/10.3390/prosthesis2020011>.
15. Rodriguez-Contreras, A.; Torres, D.; Rafik, B. *et al.* Bioactivity and antibacterial properties of calcium- and silver-doped coatings on 3D printed titanium scaffolds. *Surf Coat Technol* **2021**, *421*, 127476, <https://doi.org/10.1016/j.surfcoat.2021.127476>.
16. Mohazzab, B.F.; Jaleh, B.; Fattah-alhosseini, A.; Mahmoudi, F.; Momeni, A. Laser surface treatment of pure titanium: Microstructural analysis, wear properties, and corrosion behavior of titanium carbide coatings in Hank's physiological solution. *Surf. Interfaces* **2020**, *20*, 100597, <https://doi.org/10.1016/j.surf.2020.100597>.
17. Chung, Y.H.; Chen, T.C.; Lee, H.B.; Tsay, L.W. Effect of micro-shot peening on the fatigue performance of aisi 304 stainless steel. *Metals* **2021**, *11*, 1408, <https://doi.org/10.3390/met11091408>.
18. Khajehmirza, H.; Heydari Astaraee, A.; Monti, S.; Guagliano, M.; Bagherifard, S. A hybrid framework to estimate the surface state and fatigue performance of laser powder bed fusion materials after shot peening. *Appl Surf Sci* **2021**, *567*, 150758, <https://doi.org/10.1016/j.apsusc.2021.150758>.
19. Qu, S.; Duan, C.; Hu, X.; Jia, S.; Li, X. Effect of shot peening on microstructure and contact fatigue crack growth mechanism of shaft steel. *Mater Chem Phys* **2021**, *274*, 125116, <https://doi.org/10.1016/j.matchemphys.2021.125116>.
20. Pavan Satyanarayana, C.; Ratna Raju, L.; Ratna Sunil, B. Enhancing the wettability of pure titanium by shot peening for implant applications, *IOP Conf Ser: Mater Sci Eng* **2021**, *1185*, 012012, <https://doi.org/10.1088/1757-899X/1185/1/012012>.
21. Maleki, E.; Bagherifard, S.; Unal, O.; Bandini, M.; Hossein Farrahi, G.; Guagliano, M. Introducing gradient severe shot peening as a novel mechanical surface treatment. *Sci Rep* **2021**, *11*, 22035, <https://doi.org/10.1038/s41598-021-01152-2>.
22. Aliofkhazraei, M.; Macdonald, D.D.; Matykina, E. *et al.* Review of plasma electrolytic oxidation of titanium substrates: Mechanism, properties, applications and limitations. *Appl Surf Sci Adv* **2021**, *5*, 100121, <https://doi.org/10.1016/j.apsadv.2021.100121>.
23. Xue, T.; Attarilar, S.; Liu, S. *et al.* Surface modification techniques of titanium and its alloys to functionally optimize their biomedical properties: Thematic review. *FrontBioeng Biotechnol* **2020**, *8*, 603072, <https://doi.org/10.3389/fbioe.2020.603072>.
24. Thukkaram, M.; Cools, P.; Nikiforov, A. *et al.* Antibacterial activity of a porous silver doped TiO₂ coating on titanium substrates synthesized by plasma electrolytic oxidation. *Appl Surf Sci* **2020**, *500*, 144235, <https://doi.org/10.1016/j.apsusc.2019.144235>.
25. Chabuk, Q.K.N.; Al-Murshdy, J.M.S.; Dawood, N.M. Review: the surface modification of pure titanium by micro-arc oxidation (MAO) process. *Journal of Physics: Conference Series* **2021**, *1973*, 012114, <https://doi.org/10.1088/1742-6596/1973/1/012114>.
26. Hu, Y.; Wang, Z.; Ai, J.; Bu, S.; Liu, H. preparation of coating on the titanium surface by micro-arc oxidation to improve corrosion resistance. *Coatings* **2021**, *11*, 230, <https://doi.org/10.3390/coatings11020230>.
27. Li, Y.; Wang, W.; Yu, F. *et al.* Characterization and cytocompatibility of hierarchical porous TiO₂ coatings incorporated with calcium and strontium by one-step micro-arc oxidation. *Mater Sci Eng CMater Biol Appl* **2020**, *109*, 110610, <https://doi.org/10.1016/j.msec.2019.110610>.

28. Shimabukuro, M. Antibacterial property and biocompatibility of silver, copper, and zinc in titanium dioxide layers incorporated by one-step micro-arc oxidation: A review, *Antibiotics* **2020**, *9*, 716, <https://doi.org/10.3390/antibiotics9100716>.
29. Shimabukuro, M.; Tsutsumi, Y.; Nozalim, K. *et al.* Investigation of antibacterial effect of copper introduced titanium surface by electrochemical treatment against facultative anaerobic bacteria. *Dent Mater J* **2020**, *39*, 639–647, <https://doi.org/10.4012/dmj.2019-178>.
30. Venkataiah, M.; Anup Kumar, T.; Venkata Rao, K.; Anand Kumar, S.; Siva, I.; Ratna Sunil, B. Effect of grain refinement on corrosion rate, mechanical and machining behaviour of friction stir processed ZE41Mg alloy. *Trans Indian Inst Met* **2019**, *72*, 123–132, <https://doi.org/10.1007/s12666-018-1467-9>.
31. Kokubo, T.; Takadama, H. How useful is SBF in predicting in-vivo bone bioactivity? *Biomaterials* **2006**, *27*, 2907–2915, <https://doi.org/10.1016/j.biomaterials.2006.01.017>.
32. Lu, K.; Lu, J. Nanostructured surface layer on metallic materials induced by surface mechanical attrition treatment. *Mater Sci Eng: A* **2004**, *375–377*, 38–45, <https://doi.org/10.1016/j.msea.2003.10.261>.
33. Baktan, A-M.; Timus, D.; Soritau, O. *et al.* Tissue integration and biological cellular response of slm-manufactured titanium scaffolds. *Metals* **2020**, *10*, 1192, <https://doi.org/10.3390/met10091192>.
34. Pelaez, M.; Nolan, N.T.; Pillai, S.C.; Seery, M.K.; Falaras, P.; Kontos, A.G.; Dunlop, P.S.M.; Hamilton, J.W.J.; Byrne, J.A.; O'Shea, K.; Entezari, M.H.; Dionysiou, D.D. A review on the visible light active titanium dioxide photocatalysts for environmental applications. *Appl Catal B: Environmental* **2012**, *125*, 331–349, <https://doi.org/10.1016/j.apcatb.2012.05.036>.
35. Luiz da Silva, A.; Hotza, D.; Castro, R.H.R. Surface energy effects on the stability of anatase and rutile nanocrystals: A predictive diagram for Nb₂O₅-doped-TiO₂. *Appl Surf Sci* **2017**, *393*, 103–109, <https://doi.org/10.1016/j.apsusc.2016.09.126>.
36. Yang, L.; Yang, X.; Zhang, T.; Sun, R. Optimization of microstructure and properties of composite coatings by laser cladding on titanium alloy. *Ceram Int* **2021**, *47*, 2230–2243, <https://doi.org/10.1016/j.ceramint.2020.09.063>.
37. Ratna Sunil, B.; Anil Kumar, A.; Sampath Kumar, T.S.; Chakkingal, U. Role of biomineralization on the degradation of fine grained AZ31 magnesium alloy processed by groove pressing. *Mater Sci Eng: C* **2013**, *33*, 1607–1615, <https://doi.org/10.1016/j.msec.2012.12.095>.
38. Shishir, R.; Shebeer A.R.; Hanas, T. Effect of grain refinement on biodegradation and biomineralization of low calcium containing Mg–Ca alloy. *Mater Res Express* **2020**, *7*, 036501, <https://doi.org/10.1088/2053-1591/ab7718>.